Tracer kinetic models:

Extracting physiological vascular information

David L Buckley, PhD

Senior Lecturer, Imaging Science and Biomedical Engineering,

University of Manchester, Manchester, United Kingdom

1. Introduction

When a contrast agent, such as Gd-DTPA, is introduced into the blood stream of a patient its transport through the vascular system, heart and lungs and eventual excretion via the kidneys is a well-established process [1]. At the level of our imaging voxel (for example, in the centre of a breast tumor) we can only speculate as to the precise nature of the contrast agent kinetics. We can, however, form a hypothesis. The tracer kinetic model helps us to formulate such a hypothesis, provides us with the opportunity to predict the behavior of the system and subsequently test our predictions [2]. With time, like most hypotheses, our models become more complex attempting to describe the system with greater realism.

In the following syllabus contribution I will briefly summarize the derivation of several important tracer kinetic models used in both MRI research and clinical practice, highlight the latest developments in the field and identify some important limitations of the techniques and sources of error inherent in their use.

2. Building blocks

The indicator-dilution technique developed from physiological studies dating back to the 19th century and the mathematical foundations of today's models were laid in the late 1940s and early 1950s [3-5]. In the nuclear medicine community the field has matured and practitioners have employed sophisticated models in their analyses [6, 7].

Common to many of these approaches is a set of model building blocks (Fig. 1). For the purposes of this discussion the tissue may be said to be composed of plasma (vascular) and interstitial spaces separated by a semi-permeable endothelial cell layer (the capillary wall). Their fractional volumes, in ml/ml of tissue, are defined as v_p and v_e, respectively. A third compartment, mainly intra-cellular space but also composed of membranes, fibrous tissues and so on, is present but usually excludes contrast agents. A whole field of dynamic susceptibility contrast MRI has developed to measure tracer kinetics in the brain where the blood-brain barrier prevents transport of Gd-DTPA into the interstitium [8]. However, this discussion is limited to those models that incorporate capillary-tissue exchange and we may consider two principal exchange parameters: plasma flow, F_p measured in ml/min/ml tissue and capillary permeability-surface area product, PS measured in ml/min/ml tissue. A conversion to the common units of ml/min/g is achieved by the inclusion of the tissue density, g/ml [9] while a measure of whole blood volume and flow is obtained by multiplication by 1/(1 – hematocrit).

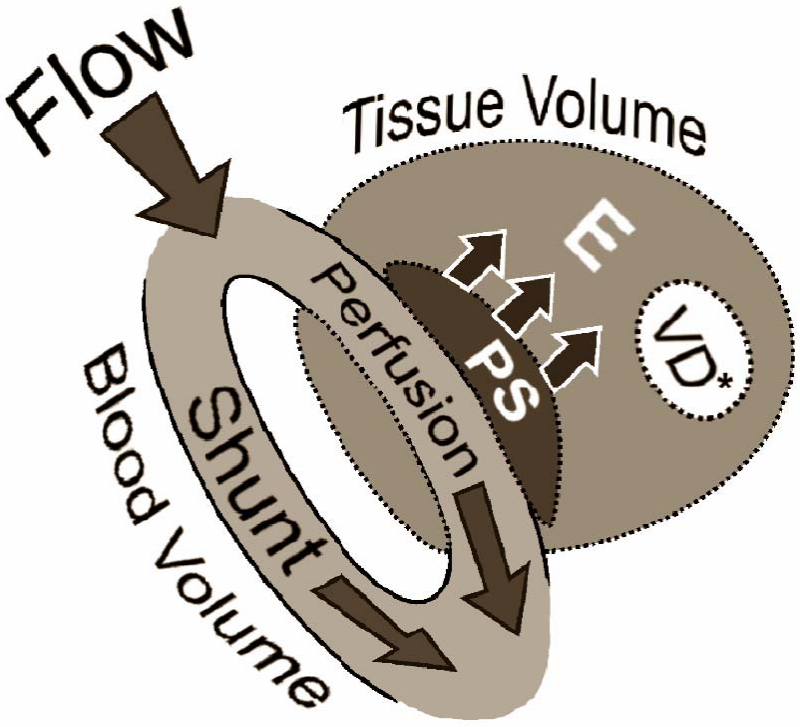

Fig. 1 – Tracer transport and exchange in tumors may be described using a set of basic building blocks. Flow (plasma flow, F_p); Shunt (flow where there is no exchange of nutrients with the tissue); Perfusion (nutritive flow); PS (permeability-surface area product); E (extracted fraction); VD* (volume of distribution – not all of the tissue volume is 'available' to the extracted tracer; in the case of Gd-DTPA this represent the interstitial volume, V_e). Modified from ref. [10].

The kinetic modeling of contrast agent distribution has a basis in the simple rate equation describing diffusive flux across a permeable membrane [11, 12]. This is determined by the difference in concentration between two compartments that are separated by the membrane and the membranes permeability. For the case of transport across the capillary wall the flux is equal to $PS(C_p - C_e)$, where P is the capillary permeability, S is the total effective surface area of the capillary wall and C_p and C_e are the concentrations of contrast agent in the plasma and interstitial spaces, respectively. In reality the concentrations of contrast agent in these compartments are not stable, the plasma concentration (and therefore capillary-tissue exchange) is dependent upon flow. The extraction fraction, E, is the relative difference between arterial and venous concentrations of contrast agent and is defined as the fractional reduction of contrast agent in the plasma during its passage through the tissue [11]. E is related to PS and F_p through the relation, $E = 1 - \exp(-PS/F_p)$. For the case of our capillary-tissue model, it can be shown that the flux across the capillary wall may be defined as $EF_p(C_p - C_e)$. EFp is otherwise known as K^{trans} and this new flux equation leads to the two limiting cases described by Tofts et al. [13]. When $F_p \gg PS$ (thus the plasma concentration is stable), $EF_p \approx PS$ and the measured flux is related directly to permeability. Conversely, if $PS \gg F_p$ ($E \approx 1$ and the plasma concentration of contrast agent is rapidly depleted) $EF_p \approx F_p$ and measured flux is related directly to flow.

3. Compartmental models

The tracer kinetic models used in most MRI studies to date are essentially based upon a modified version of Kety's original approach in which the plasma input function is convolved with the tissue impulse response derived above to arrive at an estimate of the whole tissue concentration of contrast agent ($C_t(t)$):

$$C_t(t) = K^{\text{trans}} \int_0^t C_p(t') \exp\left(\frac{-K^{\text{trans}}(t-t')}{v_e} \right) dt' \quad (1)$$

The techniques described in the early 1990s by both Larsson and Tofts follow this pattern [14, 15]. Brix et al. used the same principles [16] and common to all three approaches is the calculation of the rate constant k_{ep} (= K^{trans}/v_e) [9]. The differences between these techniques are in the details of their individual measurement schemes. With baseline estimates of T_1 and independent estimates of $C_p(t)$, they broadly reduce to the same form [17]. All require dynamic imaging following the administration of contrast agent for a time period of a few minutes or more (until equilibrium between plasma and interstitial contrast agent concentrations is achieved). Absolute estimates of K^{trans} can only be obtained when the dynamic imaging is accompanied by an estimate of baseline T_1.

What is conspicuously neglected in this model is the contribution to the signal from contrast agent in the vascular space, v_p, of the tissue. This has long been recognized in PET studies [18] and explicitly modeled in the popular Patlak approach to data analysis [19]. However, to accurately model the effects of such a contribution it is important to know the concentration of contrast in the feeding arterial system. That is, an arterial input function (AIF) must be measured. A number of investigators have developed methods to achieve this in animals [20, 21] and humans [22, 23] and a simple extension of equation 1 allows its incorporation:

$$C_t(t) = v_p C_p(t) + K^{\text{trans}} \int_0^t C_p(t') \exp\left(\frac{-K^{\text{trans}}(t-t')}{v_e} \right) dt' \quad (2)$$

This has the added benefit of providing a subject-specific AIF rather than an assumed form [15] increasing the accuracy of parameter estimates (provided the AIF is accurately measured). This model spans the fields of PET, contrast-enhanced CT and MRI and represents a popular standard for tracer kinetic analysis. An interesting limiting case for this model occurs when contrast agent transport is largely one way (e.g. in the early phases of tissue enhancement). In this case, the interstitial volume is neglected and a simplified version of equation 2 may be derived [19]:

$$C_t(t) = v_p C_p(t) + K^{\text{trans}} \int_0^t C_p(t') dt' \quad (3)$$

4. Distributed parameter models

Compact and relatively straightforward to fit, equation 2 provides a useful tool for the hypothesis-driven analysis of contrast-enhanced data. However, it lacks an important characteristic, the isolation of flow as a separable parameter. Considerable confusion has arisen in recent years with some investigators describing their K^{trans} values as measures of "permeability" and others as measures of "perfusion". While these two examples represent limiting cases without *a priori* information such a designation is premature. There has subsequently been considerable interest in developing methods to isolate flow and PS-product.

This has taken on added significance in the last couple of years with the introduction of commercial software addressing this issue directly. For example, GE Healthcare provides software associated with its CT workstation products called *CT Perfusion 2* and *CT Perfusion 3*. While it's not clear exactly how the tracer kinetics modeling is undertaken (this is a commercial product), a distributed parameter model lies at its heart. Numerous clinical groups have started using this software and a number of papers have now appeared in the literature reporting flow and PS values obtained from dynamic contrast-enhanced CT acquisitions [24-27] and emphasizing some of the complications inherent in using such complex techniques [28-30].

As with the compartmental models, distributed parameter models were pioneered very early [4, 31, 2] and have been tested in PET [6], CT [32] and MRI studies [33-35]. Central to their foundation is the concept of a measurable tissue transit time. That is, the contrast agent takes a finite time to transit the vascular volume of the tissue (= v_p/F_p) and we are able to measure this with our imaging system. Typically this transit time will be on the order of seconds and this places an increased strain on image acquisition requiring sampling intervals on the order of 1 or 2 s. However, the transport of contrast agent to the tissue during this initial period is solely due to tissue flow (i.e. extravasation may or may not occur in this initial phase; this can't be established until the tracer begins to appear in the venules) [36]. Thus the early phase of enhancement provides information about flow alone and this, combined with late phase K^{trans} estimates, can be used via the Renkin-Crone relation to extract estimates of PS. When the transit time is on the order of a few seconds (such as in the normal brain), measurement precision is limited; very few data points can be acquired in this time. However, transit time may be significantly longer in other tissues. MRI studies of the prostate gland using a sampling interval of 2.3 s [35] have provided estimates of flow and PS with acceptable precision (coefficient of variation 19% and 28%, respectively [unpublished data]). The transit time estimated in prostate tumors was ~ 20 s and this reflects the relatively low blood flow to these cancers combined with a large blood volume. While these distributed parameter models have yet to be fully validated in a clinical setting, the prostate results compare extremely well with the current gold standard, H_2O-15 PET. In a study of 11 tumor-bearing prostates, Inaba used water PET to estimate a mean flow across a whole prostate gland region of 29 ml/min/100 ml [37]. The mean value in 9 normal prostates was 16 ml/min/100 ml. The compares with MR estimates of blood flow made in regions of interest encompassing prostate tumor of 36 ml/min/100 ml and normal prostate peripheral zone of 13 ml/min/100 ml. Allowing for the partial volume averaging of central gland inherent in the PET regions, these numbers are remarkably consistent. Furthermore, the same MR data provides estimates of blood volume, PS-product and interstitial volume.

Of course, the additional complexity of the distributed parameter model makes data fitting a non-trivial problem [38] and the more complex the model the more important it becomes for the investigator to interpret their results judiciously [33]. Nevertheless, these studies provide exciting new results and will surely prick the interest of the MR community in much the same way as their introduction into the broader CT community has shown.

5. Limitations and sources of error

There are a myriad of potential pitfalls in the acquisition of dynamic contrast-enhanced MRI data and I won't attempt to cover these here other than to emphasize the importance of acquiring good quality, artifact-free data with an appropriate spatial, temporal and contrast resolution. A very

common mistake is to neglect the influence of blood hematrocrit and this must be incorporated to avoid systematic errors in parameter estimates (e.g. the investigator needs to be clear about whether they are quoting plasma or whole blood flow). Similarly, the density of the tissue examined is important if tracer kinetic parameters are quoted per unit mass of tissue [9]. Without discussing these issues further, it is worth emphasizing that considerable debate surrounds the issues of water exchange (whether T1 is really an appropriate measure of Gd-DTPA concentration) [39] and the relaxivity of Gd-DTPA in plasma and tissue [40].

When it comes to analyzing your data using a tracer kinetic model a number of issues should be considered. Is the model appropriate and not over-parameterized? Data from a slow enhancing multiple sclerosis lesion should not require the same level of model sophistication as a lung tumor. Conversely, the rim of a rapidly enhancing glioma may have a significant vascular component and estimates of K^{trans} made using equation 1 may be inaccurate [38]. As noted above, data fitting is not a trivial problem even with the simplest model. Delay and dispersion of the AIF is common [41] and correlation between parameters and error in their estimates should all be considered [33].

6. Summary

Tracer kinetic models can play a major role in the characterization of tumors, help provide prognostic information and assess the progress of treatments. Importantly, they can be used to test hypotheses and provide specific physiological insight. These techniques have been used for many years in the PET and CT communities and a considerable body of literature is available to help expedite their introduction into a variety of MR applications. They are not without their limitations and the results must be interpreted with caution but as tools for the study of cancer and its treatment they are invaluable.

Recommended Reading

Book:

A. Jackson, D.L. Buckley, G.J.M. Parker, Editors.
Dynamic Contrast-Enhanced Magnetic Resonance Imaging in Oncology
Springer-Verlag – Medical Radiology Series (2005).

Review articles:

P.S. Tofts
Modeling tracer kinetics in dynamic Gd-DTPA MR imaging
J Magn Reson Imaging **7:**91-101 (1997)

A.M. Peters
Fundamentals of tracer kinetics for radiologists
Brit J Radiol **71**:1116-1129 (1998)

References

1. Weinmann, H. J., Laniado, M. and Mutzel, W. (1984) Pharmacokinetics of Gd-DTPA/dimeglumine after intravenous injection into healthy volunteers *Physiological Chemistry and Physics and Medical NMR,* **16,** 167-172.
2. Bassingthwaighte, J. B. and Goresky, C. A. (1984) In *Handbook of physiology - Section 2: The cardiovascular system* (Eds, Renkin, E. M., Michel, C. C. and Geiger, S. R.) American Physiological Society, Bethesda, pp. 549-626.
3. Kety, S. S. and Schmidt, C. F. (1948) The Nitrous Oxide Method for the Quantitative Determination of Cerebral Blood Flow in Man - Theory, Procedure and Normal Values *J. Clin. Invest.,* **27,** 476-483.
4. Sangren, W. C. and Sheppard, C. W. (1953) A mathematical derivation of the exchange of a labeled substance between a liquid flowing in a vessel and an external compartment *Bulletin of Mathematical Biophysics,* **15,** 387-394.
5. Meier, P. and Zierler, K. L. (1954) On the theory of the indicator-dilution method for measurement of blood flow and volume *Journal of Applied Physiology,* **6,** 731-744.
6. Larson, K. B., Markham, J. and Raichle, M. E. (1987) Tracer-kinetic models for measuring cerebral blood flow using externally detected radiotracers *J Cereb Blood Flow Metab,* **7,** 443-463.
7. Kuikka, J. T., Bassingthwaighte, J. B., Henrich, M. M. and Feinendegen, L. E. (1991) Mathematical-modeling in nuclear-medicine *European Journal of Nuclear Medicine,* **18,** 351-362.
8. Calamante, F., Thomas, D. L., Pell, G. S., Wiersma, J. and Turner, R. (1999) Measuring cerebral blood flow using magnetic resonance imaging techniques *J Cereb Blood Flow Metab,* **19,** 701-735.
9. Tofts, P. S. (1997) Modeling tracer kinetics in dynamic Gd-DTPA MR imaging *J Magn Reson Imaging,* **7,** 91-101.
10. Laking, G. R., West, C. M., Buckley, D. L., Matthews, J. and Price, P. M. (2006) Imaging vascular physiology to monitor cancer treatment *Critical Reviews in Oncology/Hematology,* In Press.
11. Renkin, E. M. (1959) Transport of potassium-42 from blood to tissue in isolated mammalian skeletal muscles *Am J Physiol,* **197,** 1205-10.
12. Crone, C. (1963) The Permeability of Capillaries in Various Organs as Determined by Use of the 'Indicator Diffusion' Method *Acta Physiol Scand,* **58,** 292-305.
13. Tofts, P. S., Brix, G., Buckley, D. L., Evelhoch, J. L., Henderson, E., Knopp, M. V., Larsson, H. B., Lee, T. Y., Mayr, N. A., Parker, G. J., Port, R. E., Taylor, J. and Weisskoff, R. M. (1999) Estimating kinetic parameters from dynamic contrast-enhanced T1-weighted MRI of a diffusable tracer: Standardized quantities and symbols *J Magn Reson Imaging,* **10,** 223-232.
14. Larsson, H. B. W., Stubgaard, M., Frederiksen, J. L., Jensen, M., Henriksen, O. and Paulson, O. B. (1990) Quantitation of Blood-Brain Barrier Defect by Magnetic Resonance Imaging and Gadolinium-DTPA in Patients with Multiple Sclerosis and Brain Tumors *Magn Reson Med,* **16,** 117-131.
15. Tofts, P. S. and Kermode, A. G. (1991) Measurement of the blood-brain barrier permeability and leakage space using dynamic MR imaging. 1. Fundamental concepts *Magn Reson Med,* **17,** 357-367.
16. Brix, G., Semmler, W., Port, R., Schad, L. R., Layer, G. and Lorenz, W. J. (1991) Pharmacokinetic parameters in CNS Gd-DTPA enhanced MR imaging *J Comput Assist Tomogr,* **15,** 621-628.
17. Larsson, H. B. W. and Tofts, P. S. (1992) Measurement of Blood-Brain Barrier Permeability Using Dynamic Gd-DTPA Scanning - A Comparison of Methods *Magn Reson Med,* **24,** 174-176.
18. Gambhir, S. S., Huang, S. C., Hawkins, R. A. and Phelps, M. E. (1987) A study of the single compartment tracer kinetic model for the measurement of local cerebral blood flow using 15O-water and positron emission tomography *J Cereb Blood Flow Metab,* **7,** 13-20.
19. Patlak, C. S., Blasberg, R. G. and Fenstermacher, J. D. (1983) Graphical evaluation of blood-to-brain transfer constants from multiple-time uptake data *J Cereb Blood Flow Metab,* **3,** 1-7.
20. Shames, D. M., Kuwatsuru, R., Vexler, V., Muhler, A. and Brasch, R. C. (1993) Measurement of capillary-permeability to macromolecules by dynamic magnetic resonance imaging: A quantitative noninvasive technique *Magn Reson Med,* **29,** 616-622.
21. Checkley, D., Tessier, J. J., Wedge, S. R., Dukes, M., Kendrew, J., Curry, B., Middleton, B. and Waterton, J. C. (2003) Dynamic contrast-enhanced MRI of vascular changes induced by the VEGF-signalling inhibitor ZD4190 in human tumour xenografts *Magn Reson Imaging,* **21,** 475-82.
22. Fritz-Hansen, T., Rostrup, E., Larsson, H. B., Sondergaard, L., Ring, P. and Henriksen, O. (1996) Measurement of the arterial concentration of Gd-DTPA using MRI: a step toward quantitative perfusion imaging *Magn Reson Med,* **36,** 225-31.

23. Zhu, X. P., Li, K. L., Kamaly-Asl, I. D., Checkley, D. R., Tessier, J. J., Waterton, J. C. and Jackson, A. (2000) Quantification of endothelial permeability, leakage space, and blood volume in brain tumors using combined T1 and T2* contrast-enhanced dynamic MR imaging *J Magn Reson Imaging,* **11,** 575-85.
24. Gandhi, D., Hoeffner, E. G., Carlos, R. C., Case, I. and Mukherji, S. K. (2003) Computed tomography perfusion of squamous cell carcinoma of the upper aerodigestive tract. Initial results *J Comput Assist Tomogr,* **27,** 687-93.
25. Sahani, D. V., Kalva, S. P., Hamberg, L. M., Hahn, P. F., Willett, C. G., Saini, S., Mueller, P. R. and Lee, T. Y. (2005) Assessing tumor perfusion and treatment response in rectal cancer with multisection CT: initial observations *Radiology,* **234,** 785-92.
26. Rumboldt, Z., Al-Okaili, R. and Deveikis, J. P. (2005) Perfusion CT for head and neck tumors: pilot study *AJNR Am J Neuroradiol,* **26,** 1178-85.
27. Haider, M. A., Milosevic, M., Fyles, A., Sitartchouk, I., Yeung, I., Henderson, E., Lockwood, G., Lee, T. Y. and Roberts, T. P. L. (2005) Assessment of the tumor microenvironment in cervix cancer using dynamic contrast enhanced CT, interstitial fluid pressure and oxygen measurements *Int J Radiat Oncol Biol Phys,* **62,** 1100-1107.
28. Kealey, S. M., Loving, V. A., Delong, D. M. and Eastwood, J. D. (2004) User-defined vascular input function curves: Influence on mean perfusion parameter values and signal-to-noise ratio *Radiology,* **231,** 587-593.
29. Fiorella, D., Heiserman, J., Prenger, E. and Partovi, S. (2004) Assessment of the reproducibility of postprocessing dynamic CT perfusion data *Am J Neuroradiol,* **25,** 97-107.
30. Goh, V., Halligan, S., Hugill, J. A., Gartner, L. and Bartram, C. I. (2005) Quantitative colorectal cancer perfusion measurement using dynamic contrast-enhanced multidetector-row computed tomography - Effect of acquisition time and implications for protocols *J Comput Assist Tomogr,* **29,** 59-63.
31. Johnson, J. A. and Wilson, T. A. (1966) A model for capillary exchange *Am. J. Physiol.,* **210,** 1299-1303.
32. Cenic, A., Nabavi, D. G., Craen, R. A., Gelb, A. W. and Lee, T. Y. (2000) A CT method to measure hemodynamics in brain tumors: Validation and application of cerebral blood flow maps *Am J Neuroradiol,* **21,** 462-470.
33. Jerosch-Herold, M., Wilke, N., Wang, Y., Gong, G. R., Mansoor, A. M., Huang, H., Gurchumelidze, S. and Stillman, A. E. (1999) Direct comparison of an intravascular and an extracellular contrast agent for quantification of myocardial perfusion *International Journal of Cardiac Imaging,* **15,** 453-464.
34. Henderson, E., Sykes, J., Drost, D., Weinmann, H. J., Rutt, B. K. and Lee, T. Y. (2000) Simultaneous MRI measurement of blood flow, blood volume, and capillary permeability in mammary tumors using two different contrast agents *J Magn Reson Imaging,* **12,** 991-1003.
35. Buckley, D. L., Roberts, C., Parker, G. J., Logue, J. P. and Hutchinson, C. E. (2004) Prostate Cancer: Evaluation of Vascular Characteristics with Dynamic Contrast-enhanced T1-weighted MR Imaging--Initial Experience *Radiology,* **233,** 709-15.
36. St Lawrence, K. S. and Lee, T. Y. (1998) An adiabatic approximation to the tissue homogeneity model for water exchange in the brain: I. Theoretical derivation *J Cereb Blood Flow Metab,* **18,** 1365-1377.
37. Inaba, T. (1992) Quantitative measurements of prostatic blood flow and blood volume by positron emission tomography *J Urol,* **148,** 1457-1460.
38. Buckley, D. L. (2002) Uncertainty in the analysis of tracer kinetics using dynamic contrast-enhanced T1-weighted MRI *Magn Reson Med,* **47,** 601-606.
39. Landis, C. S., Li, X., Telang, F. W., Coderre, J. A., Micca, P. L., Rooney, W. D., Latour, L. L., Vetek, G., Palyka, I. and Springer, C. S. (2000) Determination of the MRI contrast agent concentration time course in vivo following bolus injection: Effect of equilibrium transcytolemmal water exchange *Magn Reson Med,* **44,** 563-574.
40. Stanisz, G. J. and Henkelman, R. M. (2000) Gd-DTPA relaxivity depends on macromolecular content *Magn Reson Med,* **44,** 665-667.
41. Meyer, E. (1989) Simultaneous correction for tracer arrival delay and dispersion in CBF measurements by the (H2O)-O-15 autoradiographic method and dynamic PET *J. Nucl. Med.,* **30,** 1069-1078.